

terface Part II: Film Thickness," *Trans. Inst. Chem. Eng.*, **45**, T102 (1967).

Hartland, S., "The Profile of the Draining Film beneath a Liquid Drop Approaching a Plane Interface," *Chem. Eng. Prog. Symp. Ser.*, No. 91, **65**, 82 (1969).

Hartland, S., "The Profile of the Draining Film between a Fluid Drop and a Deformable Fluid-Liquid Interface," *Chem. Eng. J.*, (London), **1**, 67 (1970).

Hartland, S., and J. D. Robinson, "A Model for an Axisymmetric Dimpled Draining Film," *J. Colloid Interface Sci.*, **60**, 72 (1977).

Hartland, S., and S. M. Wood, "The Effect of Applied Force on Drainage of the Film between a Liquid Drop and Horizontal Surface," *AIChE J.*, **19**, 810 (1973).

Hodgson, T. D., and D. R. Woods, "The Effect of Surfactants on the Coalescence of a Drop at an Interface II," *J. Colloid Interface Sci.*, **30**, 429 (1969).

Ivanov, I. B., and D. S. Dimitrov, "Hydrodynamics of Thin Liquid Films: Effect of Surface Viscosity on Thinning and Rupture of Foam Films," *Colloid Polym. Sci.*, **252**, 982 (1974).

Ivanov, I. B., B. Radoev, E. Manev, and A. Scheludko, "Theory of the Critical Thickness of Rupture of Liquid Films," *Trans. Faraday Soc.*, **66**, 1262 (1970).

Jeffreys, G. V., and J. L. Hawksley, "Coalescence of Liquid Droplets in Two-Component-Two-Phase Systems: Part 1. Effect of Physical Properties on the Rate of Coalescence," *AIChE J.*, **11**, 413 (1965).

Lang, S. B., and C. R. Wilke, "A Hydrodynamic Mechanism for the Coalescence of Liquid Drops. I. Theory of Coalescence at a Planar Interface," *Ind. Eng. Chem. Fundam.*, **10**, 329 (1971).

Lee, J. C., and T. D. Hodgson, "Film Flow and Coalescence-I. Basic Relations, Film Shape and Criteria for Interface Mobility," *Chem. Eng. Sci.*, **23**, 1375 (1968).

Murdoch, P. G., and D. E. Leng, "The Mathematical Formulation of Hydrodynamic Film Thinning and its Application to Colliding Drops Suspended in a Second Liquid-II," *Chem. Eng. Sci.*, **26**, 1881 (1971).

Myers, G. E., *Analytical Methods in Conduction Heat Transfer*, p. 274, McGraw-Hill, New York (1971).

Platikanov, D., "Experimental Investigation on the 'Dimpling' of Thin Liquid Films," *J. Phys. Chem.*, **68**, 3619 (1964).

Radoev, B. P., D. S. Dimitrov, and I. B. Ivanov, "Hydrodynamics of Thin Liquid Films: Effect of the Surfactant on the Rate of Thinning," *Colloid Polym. Sci.*, **252**, 50 (1974).

Reed, X. B., Jr., E. Riolo, and S. Hartland, "The Effect of Hydrodynamic Coupling on the Axisymmetric Drainage of Thin Films," *Int. J. Multiphase Flow*, **1**, 411 (1974a).

Reed, X. B., Jr., E. Riolo, and S. Hartland, "The Effect of Hydrodynamic Coupling on the Thinning of a Film between a Drop and its Homophase," *Int. J. Multiphase Flow*, **1**, 437 (1974b).

Reynolds, O., "On the Theory of Lubrication," *Philos. Trans. R. Soc. London Ser. A*, **177**, 157 (1886).

Riolo, E., X. B. Reed, Jr., and S. Hartland, "The Effect of Hydrodynamic Coupling on the Steady Drainage of a Thin Film between a Solid Sphere Approaching a Fluid-Fluid Interface," *J. Colloid Interface Sci.*, **50**, 49 (1975).

Scheludko, A., "Thin Liquid Films," *Adv. Colloid Interface Sci.*, **1**, 391 (1967).

Wei, L. Y., W. Schmidt, and J. C. Slattery, "Measurement of the Surface Dilatational Viscosity," *J. Colloid Interface Sci.*, **48**, 1 (1974).

Manuscript received October 16, 1979; revision received December 15, 1980, and accepted April 23, 1981.

Experimental Determination of the Light Distribution in a Photochemical Reactor:

Influence of the Concentration of an Absorbing Substance on This Profile

Knowledge of the local distribution of the light energy, in a photochemical reactor in the presence of an absorbing substance which reacts at a rate of order different from one with respect to the adsorbed light intensity, is important in order to calculate the mean rate of reaction and the design of the reactor. Here we report a simple method for the determination of this profile as a function of the concentration of an absorbing substance and we compare the results obtained with the models of emission from the literature. A semi-empirical model accounting for our experimental results is presented.

A. TOURNIER and X. DEGLISE

Laboratoire de Photochimie Appliquée
Université de Nancy I
54037 NANCY Cedex, France

and

J. C. ANDRE and M. NICLAUSE

Laboratoire de Chimie Générale
E.N.S.I.C.
54042 NANCY Cedex, France

SCOPE

Photochemical reactions have been studied extensively in both university and industrial laboratories, in particular reactions of order 1 with respect to the absorbed light intensity (photonitrosation of cyclohexane, for example, Fischer, 1974) or of order $\frac{1}{2}$ such as the chain reactions of photochlorination or of photo-oxidation (Deglise, 1968; André, 1971; Tournier, 1978).

In cases where the reaction is 1st order, knowledge of the mean number of photons absorbed in the reactor per second is

sufficient to account for the rate of reaction, and moreover in general the photoreactor is designed on the basis of heat transfer phenomena (depending on the endo- or exo-thermicity of the reaction).

On the other hand, when the order is different from 1, and when the chemical reaction involves other reactions between unstable species (excited electronic states, free radicals, ion-radicals, etc. . .) only knowledge of the absorption profile allows us to account for the rate of formation of these species. Thus, the concentration of different unstable species is no longer homogeneous in the volume of the reactor, and a concentration

gradient exists which is a function of the absorption profile of the light.

This gradient depends on all the different processes of homogenization of the medium by diffusion, convection, chemical reaction and mechanical stirring. Indeed, if the mean lifetime of the unstable reactive species is long compared to mixing times, the concentration of these species will become uniform by diffusion, through mixing, out of the absorption zone. This makes knowledge of the radiation profile dispensable. The total absorption determined by a more simple way (chemical actinometry, for example) is sufficient for the study of the photoreactor. On the other hand, when the mean lifetime of the intermediate unstable species becomes too short, the spatial distributions of these species are directly related to the light absorption profile, and it becomes important to determine them.

The bibliographical study which we have carried out has allowed us to establish that, if, up to now, all the authors concerned (Cassano et al., 1967; Jacob and Dranoff, 1966; Irazoqui, 1970; Matsuura and Smith, 1970; Zolner and Williams, 1971; Hancil et al., 1972; Cerda, 1973; Roger and Villermux, 1975; Williams, 1976; Bandini et al., 1977; Costa-Lopez, 1977) agree on the interest of such a measurement, the majority of them

have only carried out calculations on the design. While photoreactors have been studied with the aid of simplified models describing the different models of light emission, the three-dimensional nature of the emission of radiation has often been neglected to the benefit of radiation emitted in the planes perpendicular to the axis of the lamp or radially with respect to the lamp.

The interest of these simplified models resides in their great simplicity of use, but in general they give an incomplete description of the physical reality.

Nevertheless, very sophisticated models of emission do exist, but they are difficult to use. In addition, the experimental verification of these models has, in general, been carried out only infrequently and only in the absence of absorbing substance (Cassano et al., 1967; Jacob and Dranoff, 1970; Williams, 1978; Sugawara et al., 1979).

For these reasons, it is interesting to carry out such a measurement in the absence and in the presence of a substance absorbing the radiations emitted by the lamp. The results of this study should provide a better understanding of the photochemical oxidation and of chlorination reactions (Deglise, 1968; André, 1971) performed in our laboratory.

CONCLUSIONS AND SIGNIFICANCE

The results of the present study indicate the partial influence of the stray reflections and the predominant influence of the stray absorptions of the exciting light by the filtering solution. The existence of these phenomena means that the models of light emission published up to now cannot be used to interpret all our experimental results.

A semi-empirical model has been developed and tries to take these stray phenomena into account and has been com-

pared satisfactorily with our experiments using the work presented here. However, our results, show clearly that the description of the emission profile at high optical densities corresponds approximately with that of the radial model. The kinetic analysis of reactions carried out in the laboratory, of which the rate is of an order different from 1 with respect to the absorbed intensity and which depends on this absorption profile can then be improved.

EXPERIMENTAL

Principle

In the numerous industrial or laboratory arrangements for photochemical reactions, one or several filters are interposed between the lamp and the solution to be irradiated. These are destined to select the active wavelengths emitted by the lamp (Fischer, 1974) and to dissipate the thermal energy. Indeed, with the exception of lasers, instrumental devices of monochromatic emission are practically non-existent and it is often useful, if not essential to isolate a band of wavelengths for measurements of quantum yield in the laboratory or to eliminate the destructive wavelengths in industrial reactions (photochemical synthesis of caprolactam for example) (Fischer, 1974).

This type of setup, Figure 1, presents the advantage of allowing the determination of the absorption profile of the light without, in principle, having to know the intensities of the different wavelengths emitted by the lamp, the molar extinction coefficients of the absorbing substance, or finally the response of the photodetector used for the measurement.

The measurement of the local light intensity in a photoreactor dictates the use of a photodetector of restricted dimensions, and having large dynamics so as to allow the measurement of the absorption profile at high optical densities.

Those used up to now, like for example microphotoreactors containing a light-sensitive solution (Williams, 1978) or the physical receptors of the photopile type, do not allow a sufficient miniaturization, we have been obliged to construct another system of measurement capable of satisfying these two conditions.

PROPOSED TECHNIQUE

Photodetector. We have used an optical fibre (Fort Company) of small diameter (0.2 mm) fixed onto a rigid support of small dimensions (glass tube of 2-mm external diameter) in order to practically eliminate all perturbations of the light profile to be studied. The optical fibre and rigid support assembly is jointly responsible for a system of reference in three-dimensions. Evidently only the extremities of the optical fibre are stripped as is shown in Figure 1a.

The choice of a long optical fiber, i.e., of several meters avoids modification of the transmission of the fiber by displacements of the rigid support in three dimensions. For the above reasons, the end of the fiber is uncovered and recovered by a diffusing sphere.

When using an optical fiber, partially uncovered or not, part of the incident rays can enter it, as is shown in Figure 1b. However, only the rays making an angle greater than the limiting angle and corresponding to total reflection in the zones which are uncovered or those which are not able to reach the other end of the fiber.

If η_o and η represent the indices of refraction of the fiber ($\eta_o = 1.5$) and of the liquid ($\eta = 1.33$), in the non-uncovered zone, this limiting angle a_o is:

$$a_o = \text{Arcsin} \frac{1}{\eta_o} = 41.81^\circ$$

and in the non-uncovered zone is:

$$a_1 = \text{Arcsin} \frac{\eta}{\eta_o} = 62.46^\circ$$

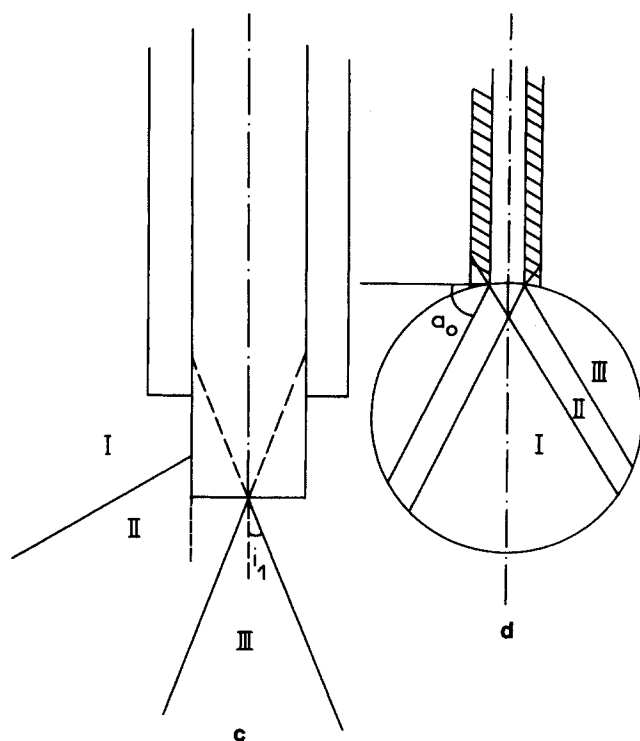
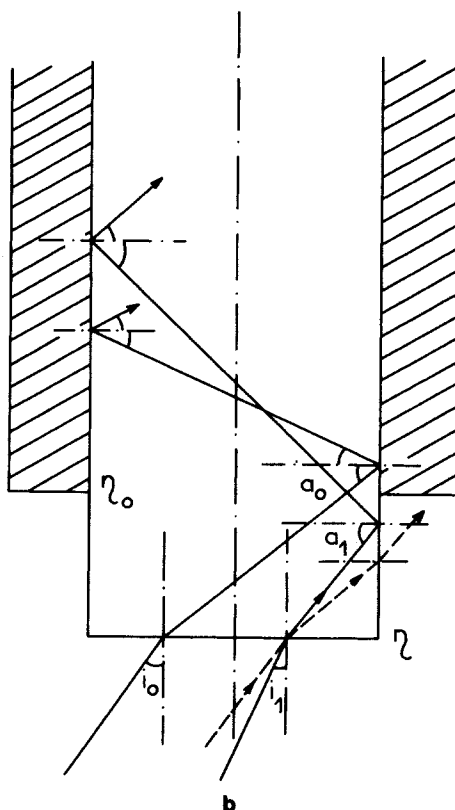
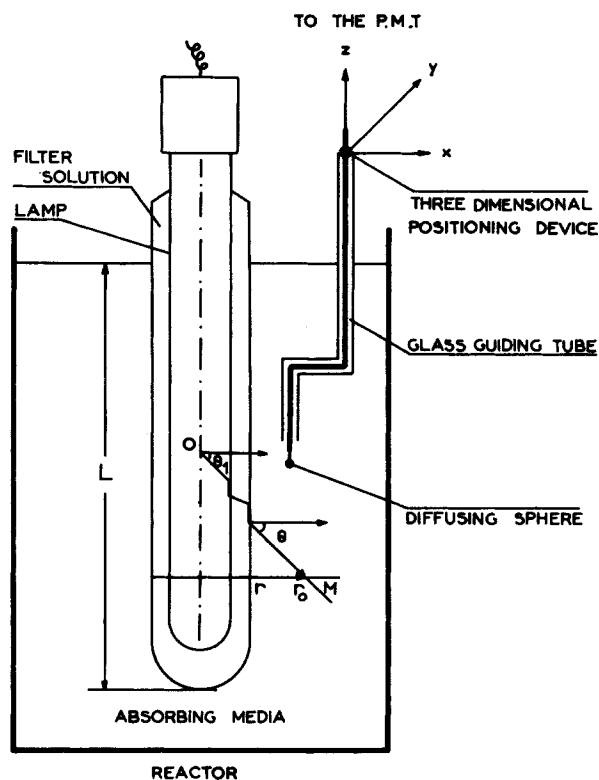


Figure 1. a) Representation of a classical experimental setup and the principle of the determination of the transmitted light intensity.

b) Demonstration of the reflected rays in the interior of the optical fiber.

c) Qualitative representation of the inhomogeneity of transfer of the light in a partially uncovered optical fiber.

Zone I: non-totally reflected rays near the other end of the fiber.

Zone II: effective zone.

Zone III: totally reflected rays near the other end of the fiber.

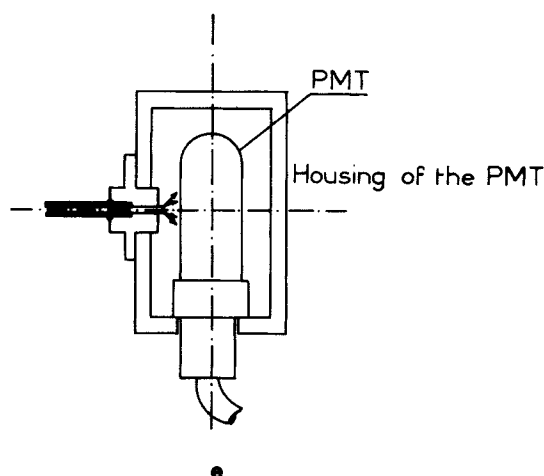
d) Visualization of the efficiency of different zones of a weakly diffusing sphere, during the transfer of luminous flux in an optical fiber.

Zone I: maximum efficiency.

Zone II: partially transmitted luminous flux.

Zone III: zero efficiency.

e) Set up of the end of the optical fiber in the PM housing.



In order to reach angles greater than a_0 or a_1 if the light rays cross the liquid/fiber interface at the cross section, orthogonal to the axis of the fiber, the maximum angles of incidence i_0 and i_1 must be:

$$i_0 = \text{Arcsin} \left(\frac{\eta}{\eta_0} \cos a_0 \right) = 41.37^\circ$$

$$i_1 = \text{Arcsin} \left(\frac{\eta}{\eta_0} \cos a_1 \right) = 24.20^\circ$$

For such restricted angles, it is not necessary to take the rate of reflection, R , which corresponds to:

$$R = \frac{1}{2} \left[\frac{\sin(i-a)}{\sin(i+a)} \right]^2 \left[1 + \left(\frac{\cos(i+a)}{\cos(i-a)} \right)^2 \right] \leq 0.02$$

with

$$a = \text{Arcsin} \left[\frac{\eta}{\eta_0} \sin i \right]$$

For light rays penetrating the fiber by its cylindrical surface, taking into account the small difference between the indices, one can consider that a large part of the light rays will cross this without being reflected. Those which are specularly reflected will have an appreciably spiral path, and will be able to reach the other end of the fiber. However, taking these slight imperfections of the light conductors into account, the rays which penetrate

practically perpendicularly to the axis of the fiber will have only a small probability of reaching the detector. Thus, with such a system there will be a very important inhomogeneity of light transfer in the fiber, Figure 1e.

To remedy this effect, one can fit an adequate optical system to the end of the fiber comprising a sphere diffusing the light and which is, as it were, a secondary light source. From the above mentioned considerations remarks, it is best to choose a sphere, sufficiently diffusing so that the incident light is diffused several times in any direction of space, which allows us to consider, to a first approximation that each ray reaching this sphere, has about the same probability of effectively entering ($a > a_0$) the conductor, and consequently of reaching the other end of the fiber.

In fact, if the diffusion of the light in this sphere is too small, there will be at most a change of direction of the light and consequently there will be, Figure 1d, zones of the sphere which will be illuminated but which will not contribute to the light transmitted at the exit. To reduce the contribution of these illuminated zones in which the efficiency of transfer is zero, one can reduce the size of the sphere but the observation will no longer correspond to a solid angle of 4π steradians.

Having taken all these considerations into account, our choice is reduced to using a diffusing sphere, which is sufficiently small so that the measured profile of light transmission is the real profile, unperturbed by the thickness of the sphere, but sufficiently large to gather the light within a large solid angle. Experimentally, we have made a sphere of about 0.5 mm diameter with the aid of a rubber solution (made by Sanford Corp., U.S.A.) adapted to optical measurements reported in the present article.

The other end of the fiber is also uncovered and penetrates the housing of a photomultiplier tube, Figure 1e.

The mean apparent optical density across a diameter is of the order of one (determined from the solution and knowing the content of dry product). This product has the advantage for other studies in being nonabsorbent up to wavelengths of around 300 nm.

For the experiments reported here, we used a home-made housing (cf., Figure 1e) with a PMT 1P28 (HAMAMATZU) with 9 dynodes supplied with 900 V using a standard power supply with neons as stabilizers.

The electrical signals are measured by means of calibrated load resistors, in the range between 100 and 10 k Ω . In all cases, the electrical measurements are carried out with a precision greater than 1% with a practically negligible dark current.

This thus provides a measuring system sensitive to the radiations emitted in practically all space, i.e., 4π steradians. Taking into account the large dynamics of the PMT this measuring system satisfies the conditions defined earlier.

REMARK

By removing the chemical filter placed between the lamp and the solution to be irradiated, and placing it between the fiber and the PMT, this photodetector can also be used to measure the light distribution in the photoreactor for the different wavelengths emitted by the lamp. This type of setup has not been used in the present work, as it does not correspond to the conventional working conditions of photoreactors.

Reactor Filter and Absorbing Solution

The photoreactor is a glass cylinder 120 mm diameter, and 230 mm high, the inside of which is coated with black paint to suppress the stray reflections coming from the lamp and from the outside (non-filtered light) which considerably perturbed our first attempts to determine an emission model discussed later. The light source is a cylindrical low pressure mercury vapour lamp mark "Ultra Violet Products" from which we succeeded in selecting two close radiations, 404.7 and 435.8 nm with the aid of a chemical filter $\text{CuSO}_4 \cdot \text{NH}_4\text{OH}$. (Murov, 1973).

The transmission curve of the filter is shown in Figure 2a. The necessity of using two emission radiations obliged us to search for a substance soluble in water and absorbing with practically the same molar extinction coefficient ϵ at 404.7 and 435.8 nm in order to study the absorption profiles. We chose a dye, quinoline yellow, characterized by the absorption spectrum reproduced in Figure 2b, and which, moreover, shows a non-perturbant fluorescence emission.

However, as is shown in Figure 2a, the filter does not completely eliminate the mercury doublet at 366 nm (maximum transmission 0.63%). This radiation being only slightly absorbed by quinoline

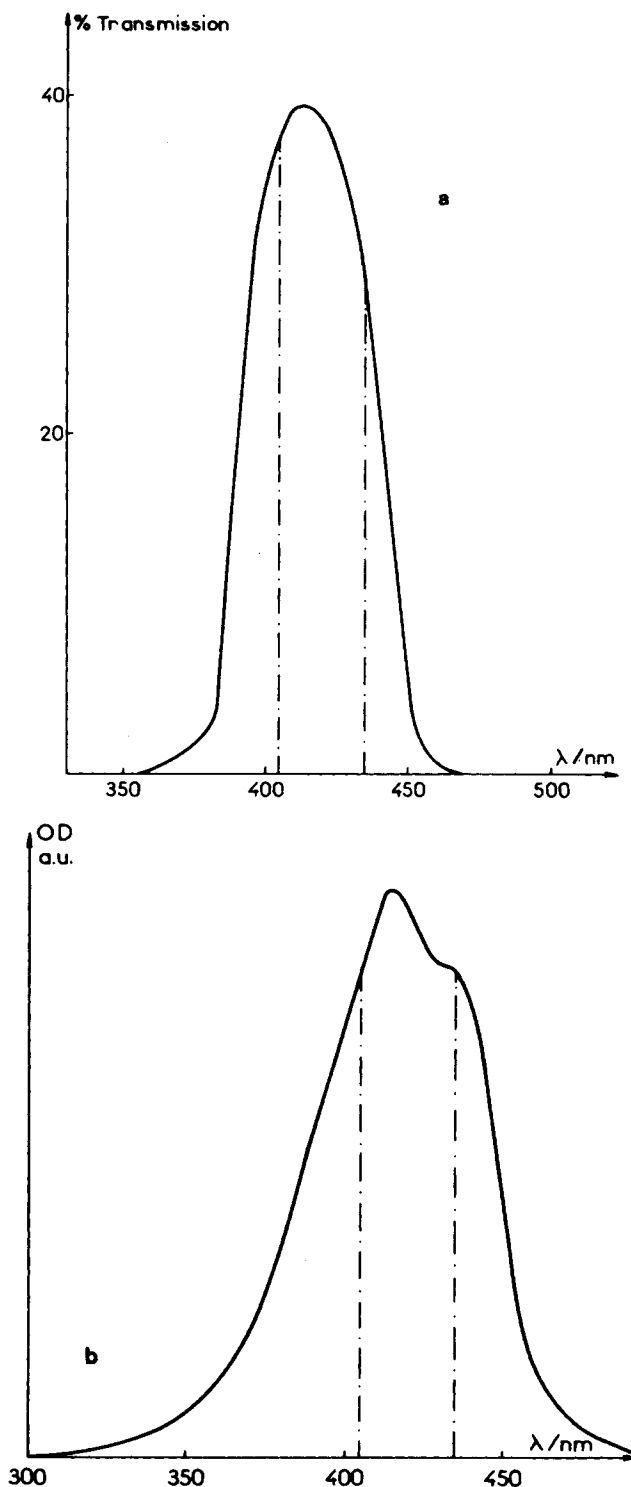


Figure 2. Curve of the transmission of the filter $\text{CuSO}_4 \cdot \text{NH}_4\text{OH}$.
b) Absorption spectrum of quinoline yellow in aqueous solution.

yellow (O.D. 0.246 at 436 nm) leads us to expect to find values in excess of the real values for high dye concentrations; the larger the distance of the diffusing sphere from the lamp, the larger will be this systematic error.

The calculation of the contribution of this radiation to the measurement of the luminous intensity has been carried out in Appendix I. It can be shown that the correction of the luminous intensity is significant only for values of the product $\mu(r - r_0)$ greater than 1.5 (cf., Table 1) (μ then corresponds to absorption coefficient, and $(r - r_0)$ to the distance from a point on the reactor to the lamp). (This correction will be applied to the data in the follow-up to this work.)

TABLE 1. CORRECTION OF LUMINOUS INTENSITY.

$\mu(r-r_o)$ 404/7 and 435.8 nm	$\mu(r-r_o)$ 366 nm	Correction Factor, f $I_{real} = f I_{measured}$
0.5	0.12	0.99
1	0.24	0.97
1.5	0.36	0.92
2	0.48	0.83
2.5	0.60	0.67

Control and Limits of the Apparatus

A control of the experimental setup has been carried out by a verification of the Beer-Lambert law, on excitation by a parallel monochromatic beam of an aqueous solution of cochineal red (O.D. 0.284 for a 1-cm path length) contained in a reactor with parallel walls of 5-cm thickness (cf., Figure 3a).

The monochromatic beam is obtained by selecting the emission wavelength 480 nm of a 150-W xenon lamp with the aid of a monochromator (FOCI), and using a slit width of 20 nm.

Under these given experimental conditions, we have determined the absorption profile of the light by moving the end of the optical fiber in a plane, longitudinal with respect to the reactor. The profile thus obtained is in perfect agreement with that forecast by the Beer-Lambert law for radial emission (cf., Figure 3b).

The precision of the luminous intensity measurements is limited by the following phenomena:

- Subsidence of non-filtered stray light
- Non-negligible volume of the diffusing sphere
- Finally, difficulty of imposing a perfectly radial path with respect to the lamp on the support for the optical fiber

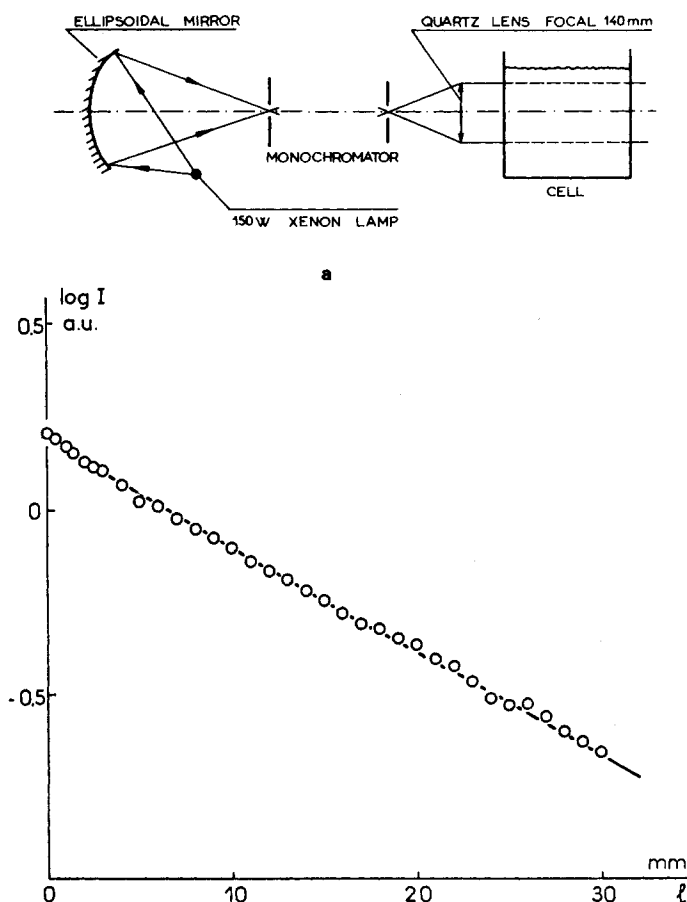


Figure 3. a) Experimental set up for testing the photodetector in a planar reactor.

b) Profile of the distribution of the light in a planar reactor in the presence of cochineal red.

Taking into account the great reliability of the optical fiber-PM ensemble, the reproducibility of the measurements will be a function only of the quality of the localization of the optical fiber with respect to the lamp, either during the reading (± 0.1 mm) or during the mechanical positioning (± 0.5 mm).

In practice, the experimental setup allows measurements of transmitted light intensity, with a good accuracy up to optical densities of about 3 for 1 cm of optical pathlength.

RESULTS

Results Obtained in the Absence of an Absorbing Substance

First of all, we have determined the profile of the light intensity in the absence of absorption, by filling the photoreactor with distilled water. The optical fiber has, therefore, been moved on a radial trajectory with respect to the lamp, from the sheath of the filter up to a pathlength of 31 mm. The results obtained are shown in Figure 4.

Taking into account the inaccuracy which exists in the measurement for the points close to the filter walls, this curve coincides perfectly with that calculated from the hypothesis of radial emission (LSPP model, Dolan et al., 1965; Harris and Dranoff, 1965; Hill and Felder, 1965; Cassano and Smith, 1966; Cassano, 1968; Irazoqui et al., 1970).

In addition, in order to evolve a design for our photoreactor we have tried to determine the theoretical model of emission which gives the best possible representation of the assembly consisting of the UV lamp and chemical filter.

In order to do this, we have studied the distribution of light intensity obtained by applying to the outside wall of the filter a mask of black adhesive substance in which we have cut out a circular window sufficiently large so that the sensitivity of the measurement is acceptable, and sufficiently narrow so that one can consider its height as negligible compared with the distances between the filter and the collecting sphere. Experimentally, a value of 2 mm satisfies these two conditions. The aperture of the window has been chosen large enough to avoid, the solid angle at which the window is seen by the end of the optical fiber being too large, and we have measured the transmitted intensity by displacing the optical fiber on a trajectory parallel to the axis of the lamp, to a distance of 17 mm from the filter.

The profile of the distribution of the light obtained is shown in Figure 5. The results of this curve will be used to establish the semiempirical model of emission presented later.

Results Obtained in the Presence of Quinoline Yellow

After taking the mask away from the filter, and by moving the optical fiber on a radial trajectory with respect to the lamp, we have determined the light distribution profile in the presence of an absorbing substance.

On addition of quinoline yellow to the solution present in the photoreactor, we have carried out measurements of the optical density varying from 0 to 2.1 for 1-cm optical pathlength; optical densities were measured with a Cary 15 UV/visible spectrophotometer.

The profiles obtained are shown in Figures 6a and 6b. The modelization of these curves will be carried out later.

DISCUSSION

Different Types of Emission Models

As the majority of industrial photoreactors are of the immersed lamp type, numerous authors have tried to schematize the profile of the light distribution in an annular space. A certain number of theoretical models have thus been developed, with hypotheses based on the following:

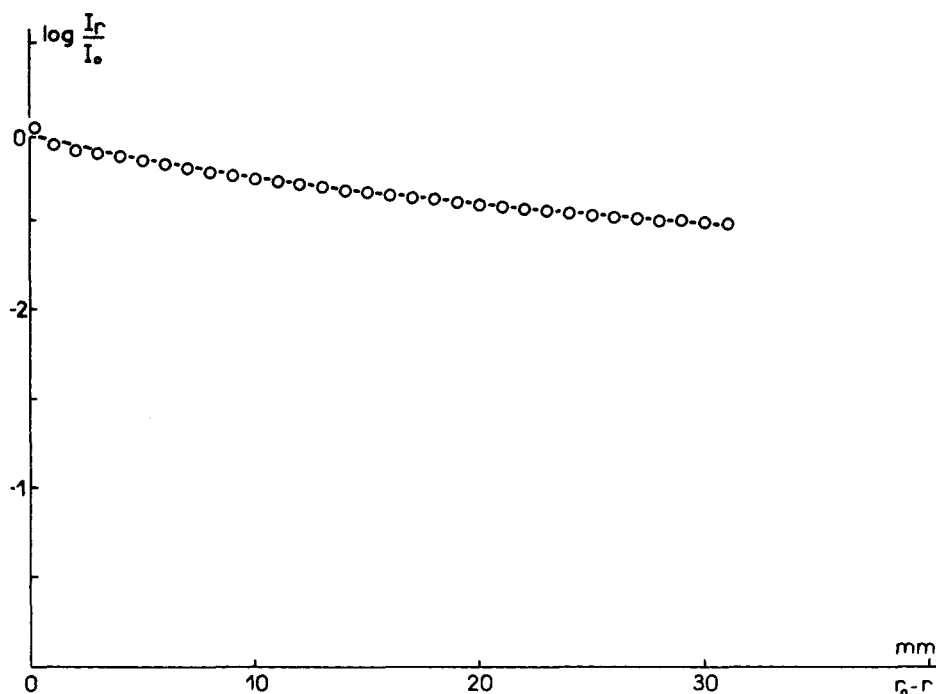


Figure 4. Profile of the distribution of the light on a radial trajectory in the absence of a substance absorbing the radiations 404.7 and 435.8 nm.

- The light emitted by the source is supposed monochromatic
- The phenomena of reflection, refraction, diffusion and diffraction of the light are neglected
- The light source follows the Lambert law, or emits with the same probability in all directions of space
- The absorption coefficient of the liquid is supposed independent of the direction of propagation of the light rays (homogeneous and anisotropic fluid)

Radial Model (LSPP Model). In this model, one supposes that the lamp is of infinite length and that all the light rays are radial with respect to the lamp. At a distance r from the axis of the lamp, the flux per unit length of the cylinder is:

$$2\pi r I_r = 2\pi r_0 I_{r_0} e^{-\mu(r - r_0)}$$

where μ represents the product of the concentration of absorbing substance and the molar extinction coefficient at the wavelength being considered, that is:

$$I_r = \frac{I_{r_0} r_0}{r} e^{-\mu(r - r_0)} \quad (1)$$

This model is evidently very easily applied but gives a poor *a priori* explanation of the physical reality.

Two Dimensional Model. Depending on the type of photo-reactor, several models of two-dimensional radiation have been developed. In the case of the cylindrical reactor the authors (Matsuura and Smith, 1970; Zolner and Williams, 1972; Roger and Villiermaux, 1975) suppose that the light rays are exclusively situated in a plane perpendicular to the axis of the reactor and that in this plane, the wall emits according to Lambert's law. For the design of annular reactors, Jacob and Dranoff (1970) assimilate the light source as a straight line each point of which emits light rays in all directions (LS model).

Under these conditions, the law defining the absorption profile, at mid-depth of reactor, is written with the notations of figure 7a:

$$I\left(r, \frac{L}{2}\right) = \frac{2I_{r_0} r_0}{\pi} \int_0^L \frac{\exp - \mu \rho(r - r_0)/r}{\rho^2} dz$$

with

$$\rho = (r^2 + z^2)^{1/2}$$

Three-Dimensional Model (ES model, Irazoqui et al., 1973). When the precedent models simplify the geometry of the emission of the light source, the diffused three-dimensional model will, on the contrary, take into account this geometry, with the following hypotheses:

- The emission of a photon is distributed uniformly in all the volume of the lamp
- The emission of each element of volume is isotropic
- The quantity of energy emitted by each element of volume is proportional to its volume
- Each element of volume inside the lamp is transparent to the emission of the other elements of volume

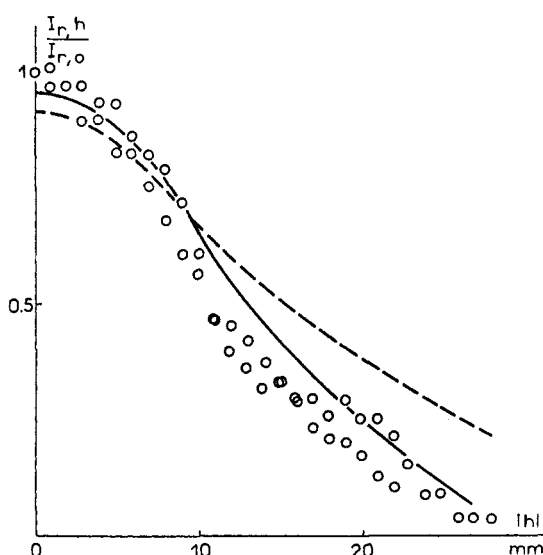


Figure 5. Profile of the distribution of the light emitted through a circular window in the absence of an absorbing substance.

- : experimental data.
- : best fit curve.
- - -: emission following the Lambert law.

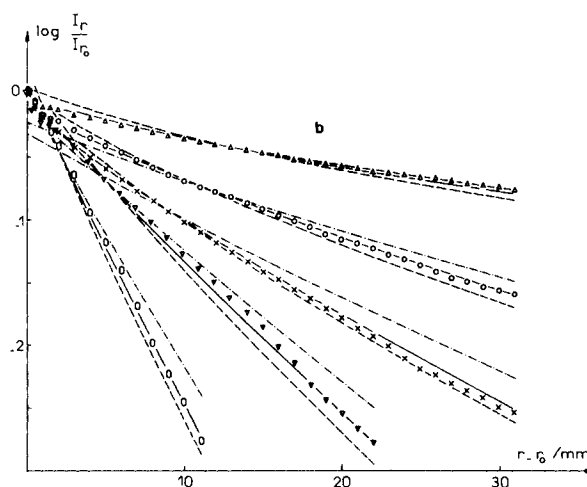
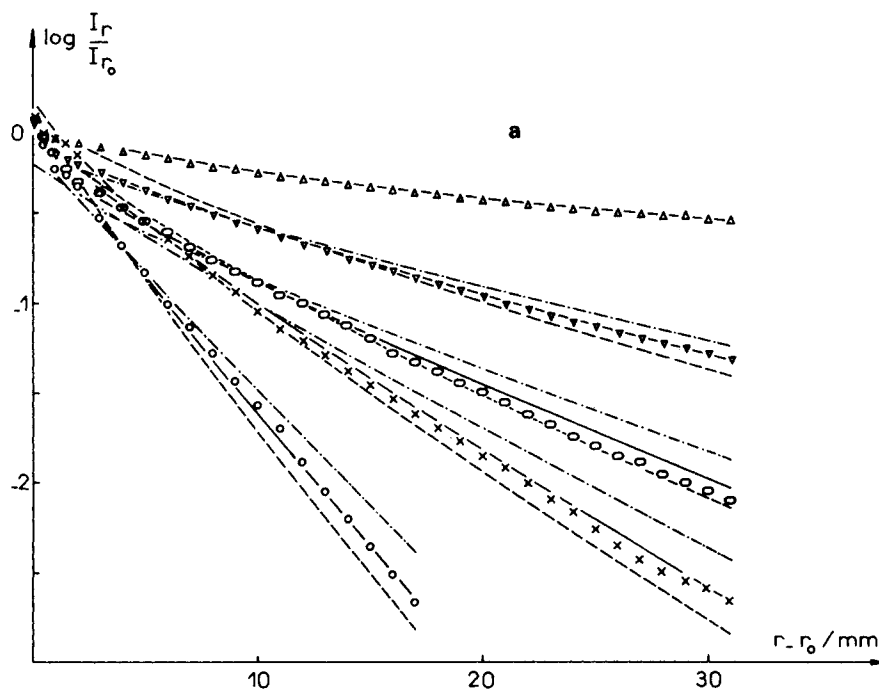


Figure 6. Presentation of some results of measurements of distribution of the emitted light in the presence of quinoline yellow.

—: our model
cvsd: two dimensional model
cvdd: radial model

Optical density for 1-cm optical pathlength	
a	b
Δ—0	Δ—0.068
▽—0.200	○—0.280
○—0.400	×—0.540
×—0.605	▽—0.940
○—1.180	○—2.10

Having taken into account these hypotheses in the absence of absorbing substances and with the notations of Figure 7b, the intensity at a point M of coordinates (z, r) is written:

$$I(r, z) = \frac{I_{r0}}{4\pi} \int_{\alpha} \int_{\varphi} \int_{\rho} \sin^2 \alpha \cos \varphi d\alpha d\varphi d\rho$$

After integration with respect to ρ and α we have

$$I(r, z) = \frac{I_{r0}}{2\pi} \int_{\varphi_1}^{\varphi_2} (r^2 \cos^2 \varphi - r^2 + r_0^2)^{1/2} (\cos \alpha_1 - \cos \alpha_2) \cos \varphi d\varphi \quad (3)$$

with

$$\alpha_1 = \tan^{-1} [(r \cos \varphi - (r^2 (\cos^2 \varphi - 1) + r_0^2)^{1/2}) / (L - z_0)]$$

$$\alpha_2 = \tan^{-1} [(r \cos \varphi - (r^2 (\cos^2 \varphi - 1) + r_0^2)^{1/2}) / (-z_0)]$$

and

$$-\varphi_1 = \varphi_2 = \cos^{-1} [(r^2 - r_0^2)^{1/2} / r]$$

It is clear that whilst this model allows us to include a large number of parameters, it appears to be difficult to handle and leads to very complex calculations in the presence of an absorbing substance. We have therefore, not tried to make use of it in the interpretation of our experimental results. [This model has been tested by Cerda,

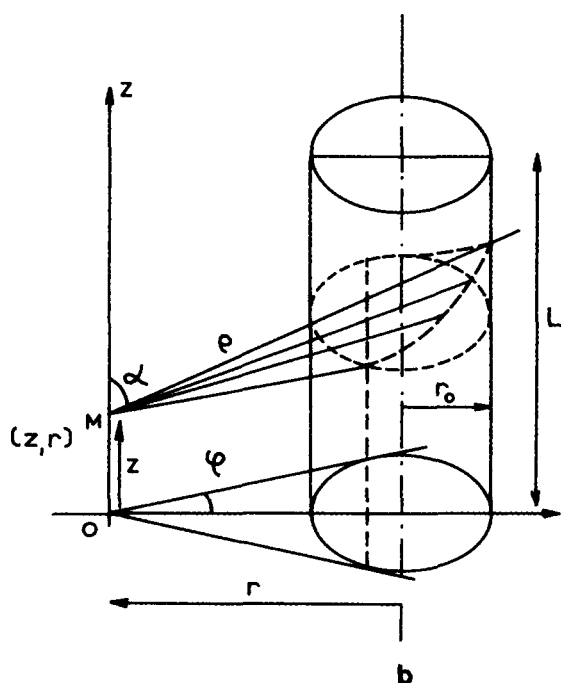
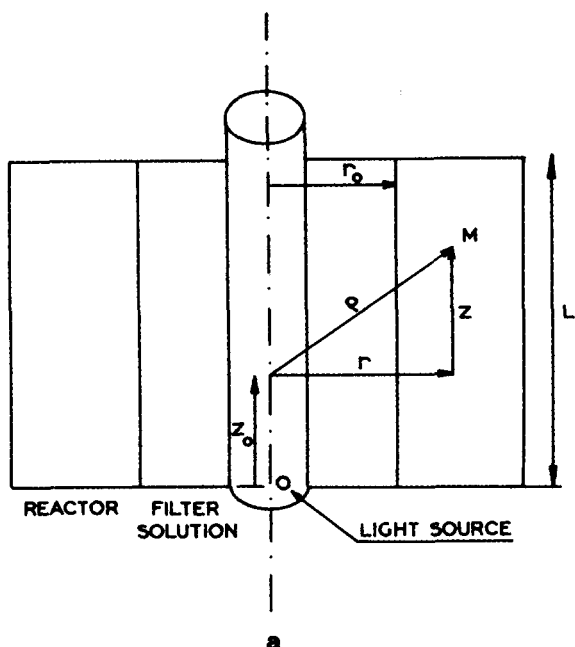


Figure 7. a) Nomenclature used for LS model.
b) Nomenclature used for ES model.

Irazoqui and Cassano (1973) in the absence of an absorbing solution.]

Comparison of Models LS and LSPP with Experiment. The comparison of our experimental results has been carried out for radial models (LSPP model) and a two dimensional (LS model). The comparison of these two models with the experimental profiles, Figure 6, allows us to draw the following conclusions:

- The two-dimensional model is in reasonable agreement with experiment for optical densities less than 1 for 1 cm optical pathlength, but deviates noticeably for higher optical densities.
- The radial model accounts very well for the experimental results for optical densities which are low (less than 0.1) or high (larger than 2). Between these two limits the correlation is no longer satisfactory. Indeed, when the optical density increases, the contribution of non radial light emissions in the profile of the light intensity drops considerably due to a larger optical pathlength, the

distribution of the light thus approaches that given by the radial model.

The interposition of a chemical filter between the lamp and the solution being irradiated, introduces significant perturbations in the profile of distribution of the light either by partial or total absorption of the radiations emitted by the lamp or by multiplication of the reflections on the glass walls.

The hypothesis according to which the light source obeys a law of simple emission is no longer verified at the exit of the filter, Figure 5. It therefore appeared to us to be interesting to establish a new model of emission for the UV lamp and chemical filter assembly from the experimental results.

On the other hand, the kinetic study of chain photoreactions, in the case of very short radical lifetimes, requires a good knowledge of the absorption profile of the light and of the rates of reaction (Tournier, 1978).

In the case of a chain reaction ($I_a^{1/2}$ law), the calculated profiles of the rate of reaction starting with the theoretical models LS and LSPP, diverge perceptibly for optical densities greater than one; for example, for an optical density of 1, the difference between the two models reaches 30%, Figure 8.

The precision of these models therefore appears to be insufficient for such kinetic studies, and only a realistic empirical model will allow us to obtain a satisfactory precision.

Semilempirical Model for Emission

When the light source has a low cross section compared with the dimensions of the photoreactor, the solid angle at which the lamp is seen from a point of the reactor remains small all along the lamp.

We have, therefore, adapted the hypothesis of a linear light source in which each point emits photons in all directions of space with the same probability. We have looked for an empirical law for light emission by fitting our experimental results with the aid of an empirical correction function in $\cos^m(\theta)$ where (θ) represents the angle of emission with respect to the normal and (m) a constant to be determined. The increase of the element of volume of emission is then attenuated by a more intense absorption of transverse radiation due to the filter, and by the phenomena of reflection and refraction at the interfaces. A value of n greater than one expresses this attenuation f .

On using the notation of Figure 9 and the experimental results shown in Figure 6, the approximate emissive volume seen by the collecting sphere is:

$$\Delta v \sim \pi e r_0 r_1$$

with:

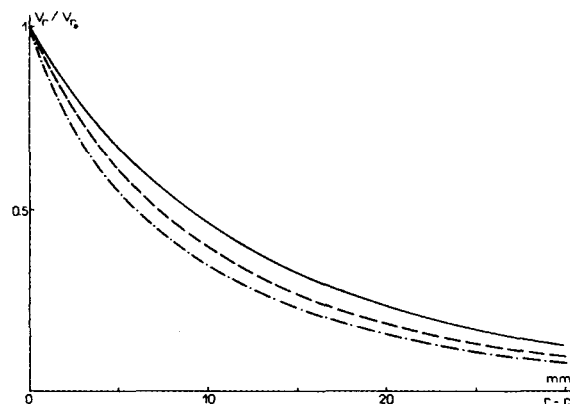


Figure 8. Influence of the model for luminous emission on the profile of the speed inside a reactor in the case of a chain reaction ($\mu = 10$).

—: LSPP model
- - - : LS model
- · - · : our model

$$e = e_o \frac{r}{r - r_o} \quad \text{and} \quad \frac{r_o}{r_1} = \cos \theta$$

i.e.

$$\Delta v \sim \pi r_o^2 e_o \frac{1}{\cos \theta} \frac{r}{(r - r_o)} \quad (4)$$

Observation at a large distance compared with z_o allows us to localize practically all the electronically excited emissive species in the vicinity of the axis and leads to a probability of collection defined by:

$$\Delta p = \frac{\pi \epsilon_o^2}{4\pi \rho^2} = \frac{\epsilon_o^2 \cos^2 \theta}{4r^2} \quad (5)$$

If $f(\theta)$ represents the coefficient of attenuation, the number of photons collected has a near multiplicative factor, expressed by:

$$\Delta n \sim \Delta v \Delta p f(\theta) = \frac{\pi}{4} e_o \epsilon_o^2 \frac{r_o^2}{r} \cos \theta f(\theta)$$

i.e.

$$\Delta n \sim K f(\theta) \cos \theta \quad (6)$$

The determination of $f(\theta) = \cos^m \theta$ is determined by the variations of $\Delta n / \cos \theta$ vs. θ . The most probable value for m determined by a parametric adjustment leads to $m = 1.86$.

Taking this result into account, it becomes possible to make a semi-quantitative determination of the variations of the transmitted intensity with the distance using the notation of Figure 9.

Contrary to the preceding treatment, under these conditions of measurement where all the lamp emits the light (absence of mask), e is no longer constant but equal to:

$$e = \Delta p \sim \frac{r}{\cos^2 \theta} \Delta \theta$$

leading to:

$$\frac{dn}{d\theta} \sim \frac{r_o}{r} \frac{f(\theta)}{\cos \theta} \exp - \mu(r - r_o / \cos \theta)$$

where μ is the product of the molar extinction coefficient and the concentration of absorbing substance.

Thus, if $I(r, \mu)$ represents the variations of the transmitted light intensity at distance r from the axis of the lamp, we shall have:

$$I(r, \mu) = 2\beta \frac{r_o}{r} \int_0^{\pi/2} \frac{f(\theta)}{\cos \theta} \exp - \mu(r - r_o / \cos \theta) d\theta$$

or

$$I(r, \mu) = 2\beta \frac{r_o}{r} \int_0^{\pi/2} \cos^{m-1} \theta \exp - \mu(r - r_o / \cos \theta) d\theta \quad (7)$$

where β is a constant.

This empirical model allows us to explain all the experimental results at whatever optical density, Figures 6a and 6b, with a rea-

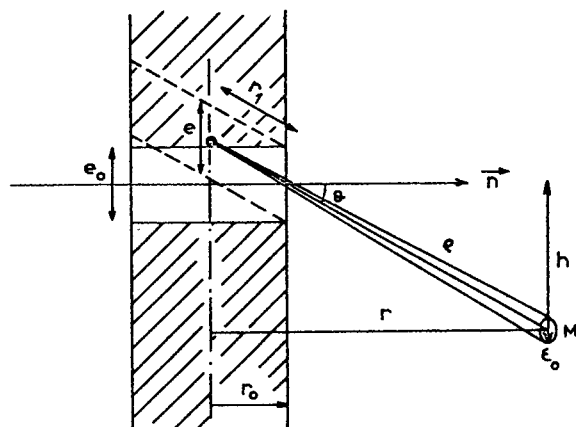


Figure 9. Notation used to define our model of emission.

sonable accuracy. The use of the correction of the emission law of the light source which was reasonable is therefore demonstrated.

In addition, the knowledge of $I(r, \mu)$ is in fact only a function of the product $\mu(r - r_o) = \nu$. Another proof of the validity of the proposed model is given in Figure 10a where we have shown the variations of $\log [r/r_o I(r, \mu)/I(r_o, \mu)]$ vs. ν for all the values of μ used thus demonstrating the agreement between the experimental results and the model described (Eq. 7).

The curve shown in Figure 10b which corresponds to the distribution of the frequency of the differences between the experimental points and the calculated point, shows that 90% of these experimental points lie in the interval 2σ , equal to an optical density of $6.6 \cdot 10^{-2}$ [$\log r/r_o I(r, \mu)/I(r_o, \mu)$].

In particular, the non-linear form of the plot of $\log [r/r_o I(r, \mu)/I(r_o, \mu)]$ vs. ν can be interpreted qualitatively by taking into account the smaller probability which the non radial radiations have of reaching the collector due to a longer optical trajectory, the larger is $\mu(r - r_o)$, the larger also is this effect. Under these conditions, it results that for larger values of μ that, as soon as we pass the zone close to the filter, only the rays emitted practically radially have the largest probability of crossing the solution. Thus, as is shown in Figure 6, we see, for the large values of r , there is an almost linear variation of $\log [r/r_o I(r, \mu)/I(r_o, \mu)]$ vs. ν with a slope practically the same as that calculated from the classical radial model.

Remarks

For the smaller values of r , corresponding to the area close to the limiting surface of the optical filter of the annular reactor, we see in Figure 5 that the relationship $I(r, \mu)$ vs. $r - r_o$ is not in as good agreement with the experimental results as it is for larger values (greater experimentally than $3-4 \text{ mm} + r_o$). This result can be

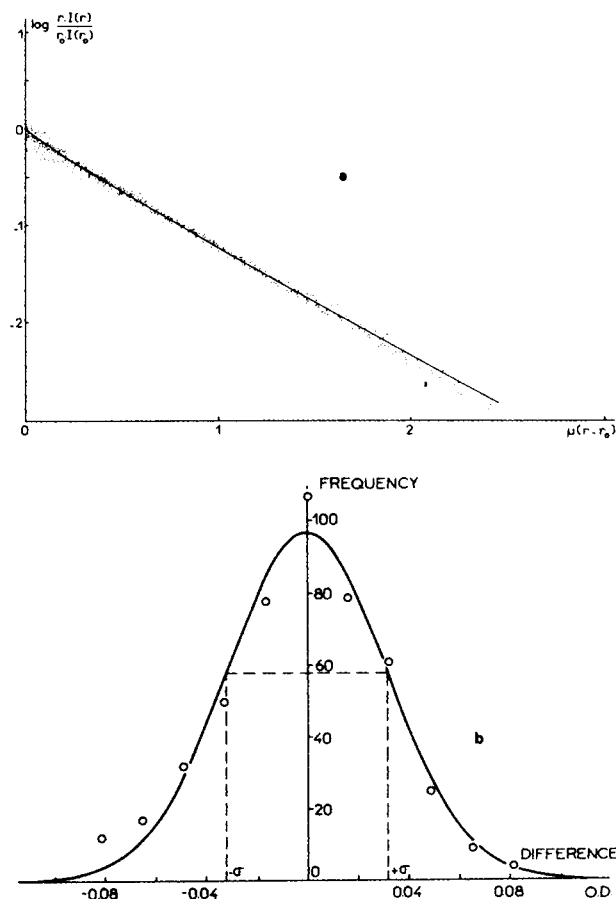


Figure 10. a) Comparison of our results with our model by dimensionless analysis.

b) Distribution of the frequency of the differences between the experimental points and the calculated point.

interpreted with the aid of the following considerations:

- Nonvalidity of the correction curve $f(\theta)$ for the low values of $r - r_o$. In fact, the simplifying hypotheses made in the determination of $f(\theta)$ concerning Δv and Δp can no longer be valid. Moreover, under these conditions, the influence of the size of the captor can intervene,
- The lamp has not got an infinitely small diameter with respect to r ,
- Difficulty of the location of the position of the captor

The modelization of the curve in Figure 5 would perhaps have been better with functions other than those in $\cos^m(\theta)$. The choice of this last function is only justified by the wish to conserve a simple trigonometric function showing a maximum for $\theta = 0$ and a minimum for $\theta = \pi/2$.

Besides, knowing the sensitivity of the method of analysis, the few approximations which had to be made can bring about non negligible errors:

- The optical densities of quinoline yellow at the two wavelengths of emission, 404.7 and 435.8 nm are not exactly the same (<10% difference). We, therefore, had to adopt a mean optical density, which at strong absorptions can partially modify the calculated profile.

APPENDIX 1

In order to try to judge the influence of the non-filtered 366 nm radiation, we can make the following hypotheses:

- The lamp has a small cross section compared with the dimensions of the photoreactor and the solid angle at which the lamp is seen from a point on the reactor remains small all along the lamp. We suppose that the source is reasonably linear and emits photons in all directions of space with the same probability.
- We neglect the phenomena of reflection, refraction and polarization of the light.

In using the nomenclature of Figure 10, the law of variation of the luminous flux I , which must reach the diffusing sphere, as a function of the angle of emission θ is written:

$$\frac{dI}{d\theta} = \frac{k}{r_o} e^{-\nu/\cos\theta}$$

where k is a constant, and ν the natural optical density of the filter. The variations of the flux I as a function of θ and ν are illustrated in Figure 11. In Table 2 we have assembled the data for the rays

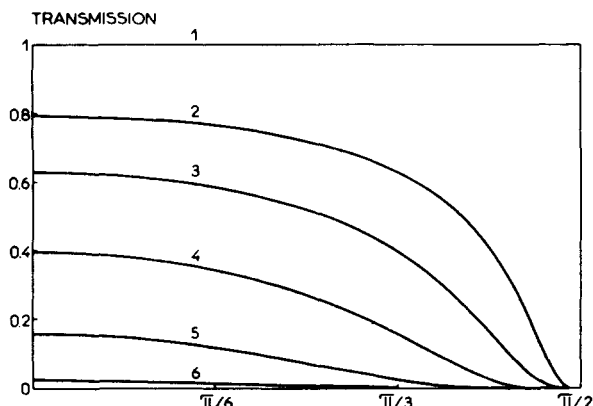


Figure 11. Variation of the luminous flux I as a function of the angle of emission.

Curve n°	ν
1	0
2	0.1
3	0.2
4	0.4
5	0.8
6	1.6

TABLE 2. DATA FOR THE LAYS AND FILTERS USED.

λ_{nm}	Energy w^*	Transmission %	λ_λ	I_w	Ratio
366	$8.1 \cdot 10^{-2}$	0.70	4.56	$1.81 \cdot 10^{-4}$	$4.0 \cdot 10^{-3}$
404.7	$5.85 \cdot 10^{-2}$	42	0.873	$1.47 \cdot 10^{-2}$	1
435.8	$1.5 \cdot 10^{-1}$	34	1.08	$3.1 \cdot 10^{-2}$	

* Murow (1973).

TABLE 3. CORRECTIONS MADE ACCORDING TO LUMINOUS INTENSITY.

Product $\mu(r - r_o)$ 404.7 and 435.8 nm	Product $\mu(r - r_o)$ 366 nm	Relative Transmitted Intensity		Stray Light Correction %
		404.7 and 435.8 nm	366 nm	
0.5	0.12	$2.29 \cdot 10^{-1}$	$2.40 \cdot 10^{-3}$	1.16
1	0.24	$6.03 \cdot 10^{-2}$	$1.83 \cdot 10^{-3}$	3.03
1.5	0.36	$1.66 \cdot 10^{-2}$	$1.36 \cdot 10^{-3}$	8.14
2	0.48	$4.57 \cdot 10^{-3}$	$0.94 \cdot 10^{-3}$	20.4
2.5	0.60	$1.32 \cdot 10^{-3}$	$0.66 \cdot 10^{-3}$	50.7

and filters used. Taking into account the hypotheses made above, the percentage of the incident light at 366 nm is about 3% in the vicinity of the entrance face of the exciting light.

Table 3 assembles the corrections that must be made to the measurement of the luminous intensity transmitted to the reactor, in order to eliminate the effect of the stray 366 nm radiation of mercury, calculated using the data given in Table 1 and from the previous experimental results.

ACKNOWLEDGMENT

A. T. and X. D. wish to express their sincere thanks to the CdF Chimie Company for its support of this work.

NOTATION

- a_o, a_1 = limiting angles for total reflection as in Figure 1b
 d_o = source diameter, length
 d_1 = lamp diameter, length
 e = slit width in the direction θ , length
 e_o = slit width on the source, length
 f = correction factor defined in Table 1
 $f(\theta)$ = coefficient of attenuation in the semi empirical model
 h = depth coordinate, length
 i_o, i_1 = maximum angles of incidence as in Figure 1b
 I_r = light intensity at distance r , energy/time
 $I_{r,h}$ = light intensity at distance r and at height h with respect to the emission slit, energy/time
 k = constant defined in Appendix 1
 K = constant defined in Eq. 6
 L = source length, length
 Δn = number of photons collected by the diffusing sphere, defined in Eq. 6
 Δp = probability of collection of photons by the diffusing sphere defined in Eq. 5
 r = radial coordinate, length
 r_o = inner radius of reactor, length
 r_1 = radius of the part of the lamp observed in the direction θ as in Figure 9, length
 Δv = emissive volume in Eq. 4
 z = coordinate of length for reactor height, length
 z_o = coordinate of length for the source, length

Greek letters

- α = spherical coordinate

ϵ	= molar extinction coefficient, length ⁻¹
ϵ_0	= radius of the diffusing sphere, length
η	= indice of refraction of the liquid
η_0	= indice of refraction of the fiber
θ	= cylindrical coordinate
λ	= wavelength of radiation, length
μ	= absorption coefficient, length
ν	= natural optical density of the filter
ρ	= cylindrical coordinate, length
σ	= standard deviation defined in Figure 10b
φ	= spherical coordinate
Ω	= solid angle

LITERATURE CITED

- André, J. C., F. Baronnet, M. Niclaude and J. Lemaire, "Nouvelle Technique d'Induction d'une Oxydation Radicalaire en Chaines, Application à l'Etude Cinétique de l'Oxydation de l'Heptanal en Phase Liquide," *J. de Chim. Phys.*, **68**, 1177 (1971).
- Bandini, E., C. Stramigioli and F. Santarelli, "A Rigorous Approach to Photochemical Reactors," *Chem. Eng. Sci.*, **32**, 89 (1977).
- Cassano, A. E., "Uso de Actinometros en Reactores Tubulares continuos," *Rev. Fac. Ing., Qca XXXVII*, **2 da P**, 469 (1968).
- Cassano, A. E., P. L. Silverston and J. M. Smith, "Photochemical Reaction Engineering," *Ind. Eng. Chem.*, **59**, 18 (1967).
- Cassano, A. E. and J. M. Smith, "Photochlorination in a tubular Reactor," *AIChE J.*, **12**, 1124 (1966).
- Cerda, J., H. A. Irazoqui and A. E. Cassano, "Radiation Fields Inside an Elliptical Photoreactor with a Source of Finite Spatial Dimensions," *AIChE J.*, **19**, 963 (1973).
- Costa-Lopez, J., "Ingenieria de Reactores Fotoquimicos," *Afinidad*, **34**, 19 (1977).
- Deglise, X., J. Lemaire et M. Niclaude, "Cinétique et Mécanisme de la Photoxydation du Butène-2-Al en Phase Liquide," *Rev. Inst. Fr. du Pétrole*, **23**, 1793 (1968).

- Dolan, W. J., C. A. Dimon and J. S. Dranoff, "Dimensional Analysis in Photochemical Reactor Design," *AIChE J.*, **11**, 1000 (1965).
- Fischer, M., "Application industrielle des synthèses photochimiques," *Actua. Chim.*, **5**, 7 (1974).
- Hancil, V., V. Schorr and J. M. Smith, "Radiation Efficiency of Photoreactors," *ibid.*, **18**, 43 (1972).
- Harris, P. R. and J. S. Dranoff, "A Study of Perfectly Mixed Photochemical Reactors," *AIChE J.*, **11**, 497 (1965).
- Irazoqui, H. A., J. Cerda and A. E. Cassano, "Análisis Racional para un Diseño Apriorístico de Reactores Fotoquímicos II," *Rev. Fac. Ing. Quím.*, **39**, 375 (1970).
- , "Radiation Profiles in an Empty Annular Photoreactor with a Source of Finite Spatial Dimensions," *AIChE J.*, **19**, 460 (1973).
- Jacob, S. M. and J. S. Dranoff, "Scale up of Perfectly Mixed Photochemical Reactors," *Chem. Eng. Prog. Symp. Ser.*, **68**, 62, 47 (1966).
- , "Light Intensity Profiles in a Perfectly Mixed Photoreactor," *AIChE J.*, **16**, 359 (1970).
- Matsuura, T. and J. M. Smith, "Light Distribution in Cylindrical Photoreactors," *ibid.*, **16**, 321 (1970).
- Murov, S. L., *Handbook of Photochemistry*, M. Dekker, Inc. (1973).
- , and J. Villiermaux, "Light Distribution in Cylindrical Photoreactors," *AIChE J.*, **21**, 1207 (1975).
- Sugawara, T., K. Omori and H. Ohashi, "Effects of Radiation Profile and Internal Light Filtering by a Product on the Reaction Characteristics in Plate Type Photoreactors," *J. Chem. Eng. Japan*, **12**, 143 (1979).
- Tournier, A., "Etude cinétique et analytique de la photochloration du Toluène," Thèse Docteur Ingénieur, Nancy (1978).
- Williams, J. A., "Experimental Observations Concerning the Diffuse, Light Intensity Distribution Model," *AIChE J.*, **21**, 1207 (1976).
- , "The Radial Light Intensity Profile in Cylindrical Photoreactors," *ibid.*, **24**, 335 (1978).
- Zolner, III, W. J. and J. A. Williams, "Three Dimensional Light Intensity Distribution Model for an Elliptical Photoreactor," *ibid.*, **17**, 502 (1971).
- , "The Effect of Angular Light Intensity Distribution on the Performance of Tubular Floro Photoreactors," *ibid.*, **18**, 1189 (1972).

Manuscript received February 12, 1980; revision received March 23, and accepted April 23, 1981.

R & D NOTES

Process Synthesis Using Structural Parameters: Further Discussion of Inequality Constraints

J. C. HEYDWEILLER

Dept. of Chemical Engineering
and Materials Science
Syracuse University
Syracuse, NY 13210

and

L. T. FAN

Department of Chemical Engineering
Kansas State University
Manhattan, KS 66506

As a result of their study on the synthesis of a small heat exchanger network, Shah and Westerberg (1977) have shown that "if the structural parameters are to be used for a synthesis problem,

and if inequality constraints are involved, the problem has to be formulated very carefully, if indeed it can be, to make it a continuous one." The purpose of this note is to show how structural parameters (Umeda et al., 1972; Ichikawa and Fan, 1973) can be used to formulate their problem in such a way as to have a continuous objective function; however, this is not to suggest that the